Stochastic process behind nonlinear thermodynamic quantum master equation. II. Simulation

Jérôme Flakowski, Marco Schweizer, and Hans Christian Öttinger*
Polymer Physics, ETH Zürich, Department of Materials, CH-8093 Zürich, Switzerland
(Dated: July 26, 2012)

We simulate a piecewise deterministic Markovian jump process that represents an unraveling of a nonlinear quantum master equation describing the evolution of a quantum subsystem in contact with a heat bath. This process relies on running ensemble averages and state vectors normalized only on average. The latter causes the normalization of a small subset of trajectories to grow exponentially resulting in numerical instability. We propose an efficient solution to this problem and illustrate the general ideas for a harmonic oscillator and a two-level system, each of them being weakly coupled to a heat reservoir. Our findings lay the foundations for a powerful simulation technique for dissipative quantum systems surrounded by general classical nonequilibrium environments.

PACS numbers: 03.65.Yz, 05.30.-d, 05.70.Ln, 02.50.Ga, 07.05.Tp

I. INTRODUCTION

In nanoscale technological applications [1] we rarely deal with perfectly isolated quantum systems. The theory of open quantum systems [2–5] provides the proper framework to study the emergence of dissipation and decoherence phenomena when a quantum subsystem starts to interact with its surroundings.

Among the numerous available methods for open quantum systems [6], many rely on linear quantum master equations for the evolution of a reduced density operator (obtained after eliminating the variables of the environment) of the Redfield [7], Lindblad [8, 9], or Caldeira-Leggett type [10, 11]. However, it has been argued that, especially when handling quantum subsystems weakly coupled to memoryless cold environments, linear equations do not lead to relaxation to the proper equilibrium state [5, 12]. Moreover, hot and noisy environments [13] as well as anharmonic oscillators [14] or composite quantum systems [15] are also problematic when employing these linear approaches. An alternative description based on a thermodynamically consistent nonlinear quantum-classical master equation [16] has recently been developed. It allows us to treat arbitrary classical nonequilibrium environments, including time-dependent ones, without giving up the Markov assumption. Moreover, the corresponding quantum master equation relaxes properly even at very low temperatures [12, 17].

As suggested in the companion paper [18], one can focus on the wave function ψ_t of the reduced Hilbert space and model its dynamics through a stochastic differential equation instead of working directly with the quantum master equation. The key ingredient of this unraveling procedure is to reproduce the evolution of the density operator $\rho(t)$ of the quantum subsystem using the covariance $\mathrm{E}\big(|\psi_t\rangle\langle\psi_t|\big)$ obtained by averaging over many realizations of a stochastic process [3]. Alternatively, one can apply a pair of stochastic processes ψ_t and ϕ_t and similarly reconstruct the density operator with $\mathrm{E}\big(|\psi_t\rangle\langle\phi_t|\big)$.

In general, two main procedures are used to generate ensembles of state vectors: The continuous quantum state diffusion technique based on Wiener processes [19, 20] and the discontinuous quantum-jump method relying on Poisson processes [21, 22]. We here rely on the latter approach which produces quantum trajectories using a smooth deterministic time evolution driven by a modified Schrödinger equation, randomly interrupted by discontinuous jumps, as described in the companion paper [18]. This approach is often equivalently described as a Monte Carlo wave function propagation [21], a stochastic Schrödinger equation or a piecewise deterministic jump process [3]. The main difference compared to standard stochastic unravelings is that the nonlinearity imposes a coupling among the different trajectories [18]. The fact that the normalization of the state vectors is conserved on average only in this process is known to lead to an exponential growth of the norm of a small number of state vectors [14, 23–25] and to generate numerical instability in long-time simulations.

We begin with a brief review of the stochastic unraveling for the nonlinear thermodynamic master equation (Sec. II). We then present the harmonic oscillator and explain how to handle numerical instabilities (Sec. III). The next section is devoted to the two-level system (Sec. IV). All simulation results are compared to the results of the deterministic approach [17]. We conclude with a few remarks and discuss some perspectives (Secs. V and VI).

II. STOCHASTIC PROCESSES

In the companion paper [18], two unravelings for the nonlinear thermodynamic quantum master equation have been constructed following a mean-field approach. We here present these stochastic processes in a form directly suited for simulations. Whereas a single operator is used for the coupling between a quantum system and its environment in [18], we here describe the equations for an

*hco@mat.ethz.ch; http://www.polyphys.mat.ethz.ch/

arbitrary number of coupling operators.

A. One-space process

In a stochastic unraveling, we represent the time evolution of the density matrix ρ of the quantum subsystem in contact with a classical environment through a stochastic process $|\psi\rangle$ in the Hilbert space of the open quantum system by means of $\rho(t) = \mathrm{E}\big(\,|\psi_t\rangle\,\langle\psi_t|\,\big)$. The time evolution of the trajectories $|\psi_t\rangle$ is given by Eqs. (7) and (8) of [18]. These two equations can be cast into the compact form

$$\begin{aligned} d\,|\psi_t\rangle \;&=\; -\frac{i}{\hbar}H\,|\psi_t\rangle\,dt + \sum_j \Lambda_j\,|\psi_t\rangle\,dt \\ &\quad + \sum_j \Big(\alpha_j\tilde{Q}_j\,|\psi_t\rangle - |\psi_t\rangle\Big)\,dN_t^j, \end{aligned} \tag{1}$$

composed of a reversible Schrödinger-type equation of motion in terms of the Hamiltonian H and an irreversible part consisting of the friction and jump operators, Λ_j and $\tilde{Q}_j$, respectively. The latter pair is present solely due to the interaction of the quantum subsystem with the environment. The continuous motion of the trajectories $|\psi_t\rangle$ is from time to time interrupted by discontinuous jumps happening in one of the various channels j associated with the jump operators $\tilde{Q}_j$. The occurrence of these jumps is modeled by the independent Poisson processes N^j with rate γ_j. Options for the choice of the free parameters α_j are discussed below.

For a proper choice of the operators Λ_j and $\tilde{Q}_j$ as well as the rate parameters γ_j, the second moment of this process reproduces the thermodynamic quantum master equation [18]. The friction operator Λ_j and jump operator $\tilde{Q}_j$ must be chosen in a complementary way

$$\Lambda_j = \frac{\gamma_j}{2}\Big(\mathbb{I} - {\alpha_j}^2{Q_j}^2 + {\alpha_j}^2\beta_j^2\left(\left[Q_j,H\right]_\rho\rho^{-1}\right)^2\Big), \tag{2}$$

and

$$\tilde{Q}_j = \left(Q_j + \beta_j\left[Q_j,H\right]_\rho\rho^{-1}\right), \tag{3}$$

where the coupling operators Q_j are given through their occurrence in the thermodynamic quantum master equation. The operators Λ_j and $\tilde{Q}_j$ are not self-adjoint, the parameters α_j can be chosen freely and the nonlinear term is defined by

$$A_\rho = \int_0^1 \rho^\lambda A\;\rho^{1-\lambda}\;d\lambda. \tag{4}$$

For a heat bath, the rates γ_j are given by

$$\gamma_j\alpha_j^2 = 2M_{\mathrm{e}}^{Q_j}(T_{\mathrm{e}}), \tag{5}$$

and the parameters β_j must be chosen as

$$\beta_j = \frac{1}{2k_{\mathrm{B}}T_{\mathrm{e}}}, \tag{6}$$

where the temperature T_{e} and the dissipation rates $M_{\mathrm{e}}^{Q_j}(T_{\mathrm{e}})$ completely characterize the heat bath and the strength of its interaction with the quantum system. For a more complex classical environment, the parameters β_j and γ_j would be given in terms of a dissipative bracket (see [18]).

For the equation of motion (1), the normalization $\langle\psi_t|\psi_t\rangle$ of the trajectories $|\psi_t\rangle$ is not preserved; however, the average $\mathrm{E}\big(\,\langle\psi_t|\psi_t\rangle\,\big)$ remains normalized to unity. We fix the still unspecified phase parameters α_j by the condition

$${\alpha_j}^2\Big[\mathrm{tr}(Q_j\rho\,Q_j) - {\beta_j}^2\mathrm{tr}\big(\left[Q_j,H\right]_\rho\rho^{-1}\left[Q_j,H\right]_\rho\big)\Big] = 1, \tag{7}$$

which implies that the average normalization of the trajectories during the deterministic evolution and the jumps are conserved separately. Optimization of the scaling parameter α_j can be achieved without breaking the stochastic formulation and can lead to more stable evolution [26]. As a consequence of the nonlinear nature of the thermodynamic quantum master equation, the appearance of the density matrix in Λ_j and $\tilde{Q}_j$ leads to a coupled evolution of the trajectories of the process. In the simulation of stochastic trajectories, the mean-field density matrix $\rho(t) = \mathrm{E}(|\psi_t\rangle\,\langle\psi_t|)$ can conveniently be calculated as a running ensemble average.

Finally, when using the Hamiltonian H as a single coupling operator Q_j, we obtain an unraveling in the mean-field spirit for Milburn-type of master equation [27] because the nonlinear term $\left[Q_j,H\right]_\rho$ vanishes. This equation then describes a non-dissipative or phase decoherence process. Otherwise, by employing the linear approximation $[Q,H]_\rho \approx \{[Q,H],\rho\}/2$, an unraveling is obtained for Caldeira-Legett-type of master equations. Moreover, for small β we recover the high temperature limit giving rise to a non-normalized Lindblad type of unraveling.

B. Two-space process

As an alternative to the stochastic process of the previous section, we can write $\rho(t) = \mathrm{E}\big(\,|\psi_t\rangle\,\langle\phi_t|\,\big)$ in terms of a pair of ket-vectors $|\psi_t\rangle$ and bra-vectors $\langle\phi_t|$ [18]. The evolution equation (1) then needs to be replaced by the following two equations:

$$\begin{aligned} d\,|\psi_t\rangle \;&=\; -\frac{i}{\hbar}H\,|\psi_t\rangle\,dt + \sum_j \Lambda_j\,|\psi_t\rangle\,dt \\ &\quad + \sum_j u_t^j\,\Big(\alpha_j\tilde{Q}_j\,|\psi_t\rangle - |\psi_t\rangle\Big)\,dN_t^j \\ &\quad + \sum_j \big(1-u_t^j\big)\Big(\alpha_j Q_j\,|\psi_t\rangle - |\psi_t\rangle\,\Big)dN_t^j, \end{aligned} \tag{8}$$

and

$$d\,|\phi_t\rangle \;=\; -\frac{i}{\hbar}H\,|\phi_t\rangle\,dt + \sum_j \Lambda_j\,|\phi_t\rangle\,dt + \sum_j \left(1-u_t^j\right)\Big(\alpha_j\tilde{Q}_j\,|\phi_t\rangle - |\phi_t\rangle\Big)\,dN_t^j + \sum_j u_t^j\Big(\alpha_j Q_j\,|\phi_t\rangle - |\phi_t\rangle\Big)dN_t^j. \tag{9}$$

The independent random variables u_t^j assume the values 0 and 1 with probability 1/2; note that they are required only at the discrete jump times of the Poisson processes. Instead of the friction operator (2), we now use

$$\Lambda_j = \frac{\gamma_j}{2}\Big[1-{\alpha_j}^2{Q_j}^2\Big], \tag{10}$$

and the coefficients β_j must be chosen as

$$\beta_j = \frac{1}{k_{\rm B}T_{\rm e}}. \tag{11}$$

The jump operators $\tilde{Q}_j$ and the rate parameters γ_j are still given by Eqs. (3) and (5), respectively.

The differences in the evolution of the pairs of bra and ket trajectories appear only in their jump parts. Whenever a jump event occurs in one of the processes N^j, for one of the two trajectories, which is selected randomly with probability 1/2, we still apply the jump operator $\alpha_j\tilde{Q}_j$, whereas the other jump is performed with $\alpha_j Q_j$. A possible choice for the free parameters α_j leading to the conservation of the overlap $\langle\phi_t|\psi_t\rangle$ on average during the deterministic and jump evolution separately is given by

$$\alpha_j^2\,{\rm tr}(Q_j\rho\,Q_j) = 1. \tag{12}$$

This alternative solution strategy based on two processes has its advantage in simpler and self-adjoint friction operators Λ_j at the expense of having to simulate two processes simultaneously. In numerical Monte-Carlo simulations of the pair of processes $|\psi_t\rangle$ and $|\phi_t\rangle$, where only a finite number of simulated samples can be used, the density matrix defined by $\rho(t) = {\rm E}\big(\,|\psi_t\rangle\,\langle\phi_t|\,\big)$ is in general not self-adjoint. Yet, this can be guaranteed without modifying the drift- and jump operators by using the symmetrized form $\rho(t) = (1/2)\ {\rm E}\big(\,|\psi_t\rangle\,\langle\phi_t| + |\phi_t\rangle\,\langle\psi_t|\,\big)$ instead.

C. Nonlinearity

The unraveling procedure requires the calculation of the nonlinear term $[Q_j, H]_\rho$ occurring in Eqs. (2), (3) and (7). For an explicit calculation, one can make use of the spectral decomposition of the density matrix $\rho = \sum_k p_k\,|\pi^k\rangle\,\langle\pi^k|$ where p_k and $|\pi^k\rangle$ are its eigenvalues and orthonormal eigenvectors. By performing the integration in Eq. (4), one obtains the following identity [17],

$$A_\rho = \sum_{k,l=1}^{n} \frac{p_k - p_l}{\ln p_k - \ln p_l}\,A^\pi_{kl}\,|\pi^k\rangle\,\langle\pi^l|\,, \tag{13}$$

where $A^\pi_{kl} = \langle\pi^k|\,A\,|\pi^l\rangle$ are the matrix elements of A in the eigenbasis of the density matrix. Note that the factor in front of A^π_{kl} possesses well defined lower and upper bounds [28],

$$\sqrt{p_k p_l} \;\le\; \frac{p_k - p_l}{\ln p_k - \ln p_l} \;\le\; \frac{p_k + p_l}{2}, \tag{14}$$

so that no problems occur for $p_k = p_l$. If p_k or p_l (or both of them) go to zero, also this factor goes to zero. Moreover, like the bounds, the factor in the middle of Eq. (14) changes monotonically with $p_k, p_l \in [0,1]$ [29].

As, in general, the eigenvectors of the density matrix change with time, they should be represented in terms of a fixed orthonormal basis. A convenient choice is the eigenbasis of the Hamiltonian or an appropriate approximation to the Hamiltonian. The matrix elements A^π_{kl} are then obtained from the matrix elements of A in the fixed basis by a time-dependent unitary transformation. To avoid the diagonalization step one could choose the eigenvalues p_k according to the aimed Boltzmann distribution at the expense of generating an approximate relaxation process.

D. Discretization of the unraveling

We give here a short recipe for handling the one and two-space unravelings (see Sec. II A and II B). The solution of Eq. (1) is a stochastic process $|\psi\rangle$ with continuous trajectories interrupted by discontinuous jumps. We seek a solution for all times t in the interval $[0,T]$, where each trajectory solves Eq. (1) for the corresponding realization of the set of independent Poisson jump processes N^j. In numerical simulations we work with discrete time points equally spaced by a time step Δt so that $0 = t_0 < t_1 < \ldots < t_s < \ldots < t_{T/\Delta t} = T$, on which we try to approximate the states of the stochastic trajectories. For computational purposes we use a finite number N of discretized trajectories $|\Psi^l\rangle$, where $l = 1,\ldots,N$. We here make use of the fact that, for weak dissipation, only a few state vectors jump whereas the others evolve according to the same deterministic equation. We group all identical trajectories into blocks $(|\Psi^b\rangle\,; N_b)$, where N_b is the number of identical state vectors $|\Psi^b\rangle$, and evolve each block as a single trajectory.

1. *Initialization procedure*

Initially, we have to produce an ensemble of state vectors that represents the initial density matrix. To do so,

we construct as many blocks $(|\Psi^b_{t_0}\rangle; N_b)$ at time t_0 as the dimension n of the Hilbert space, each of them containing N_b state vectors $|\Psi^b_{t_0}\rangle = a_b |\pi^b_{t_0}\rangle$ proportional to the eigenvectors $|\pi^b_{t_0}\rangle$ of the density matrix for $b = 1, \ldots, n$. Because we need to represent the inverse density matrix in Eqs. (2), (3) and (7) with sufficient accuracy, it is important to guarantee sufficiently large ensembles also for small eigenvalues p_b. The most natural choice is then to impose equal numbers $N_b = N/n$ for the n blocks by choosing $a_b = \sqrt{np_b}$.

2. Time-evolution

As time evolution takes place, jump events generate additional blocks shrinking the original ones. A block can also consist of a single trajectory. We then distinguish "large" blocks which have only undergone deterministic evolution (and contain the majority of the state vectors) and "small" blocks produced by jumps (and containing only a small fraction of the state vectors). To obtain the number ΔN_b of state vectors of the block $(\Psi^b_{t_s}; N_b)$ which jump at time t_s in case there is only one jump channel, we can use binomial random numbers with the number of trials being N_b (the number of elements of a block b) and the probability of jump $p = 1 - \exp(-\gamma \Delta t) \simeq \gamma \Delta t$ as probability of success in terms of the jump rate γ. Alternatively, we can approximate the number of jumps for each block b through Poisson random numbers with mean pN_b. Due to the small jump probability $p \ll 1$ the approximation is justified although $\Delta N_b > N_b$ could be obtained in principle (we would then set $\Delta N_b = N_b$, that is, all trajectories jump). In case of J multiple equiprobable jump channels, we use the total jump rate $\Gamma = \sum_j \gamma_j$ for the jump probability $p \simeq \Gamma \Delta t$ to generate the total number of jumps $\Delta N_b = \sum_j \Delta N^j_b$ of a block b with $j = 1, \cdots, J$. This total number can then be distributed among the J channels using a multinomial distribution with probability of success $p_j \simeq \gamma_j/\Gamma$ for channel j to find the different ΔN^j_b at time t_s so that the block b is split in at most $J + 1$ small blocks:

$$\begin{aligned}(\Psi^b_{t_s}; N_b) \;\rightarrow\; & \{(D\Psi^b_{t_s}; N_b - \Delta N_b), \\ & (\alpha_1 \tilde{Q}_1 \Psi^b_{t_s}; \Delta N^1_b), \cdots, \\ & (\alpha_J \tilde{Q}_J \Psi^b_{t_s}; \Delta N^J_b)\}. \end{aligned} \tag{15}$$

The new small blocks $(\alpha_j \tilde{Q}_j \Psi^b_{t_s}; \Delta N^j_b)$ containing ΔN^j_b state vectors are evolved through the application of the jump operator $\alpha_j \tilde{Q}_j$. The block $(D\Psi^b_{t_s}; N_b - \Delta N^j_b)$ containing $N_b - \Delta N_b$ state vectors is evolved with the operator $D = \mathbb{I} - (i/\hbar)\mathcal{H}\Delta t$ where $\mathcal{H} = H + i\hbar \sum_j \Lambda_j$ is the deterministic evolution operator. We reconstruct the density matrix with

$$\rho(t_s + \Delta t) = \sum_b w_b |\Psi^b_{t_s+\Delta t}\rangle \langle \Psi^b_{t_s+\Delta t}|, \tag{16}$$

where the weight of block b is defined through the value $w_b = (N_b/N) \langle \Psi^b_{t_s+\Delta t} | \Psi^b_{t_s+\Delta t} \rangle$. In this block, we can define the weight of a single state vector l_b by $w^{l_b}_b = w_b/N_b$ where $l_b = 1, \cdots, N_b$. A block disappears if it contains no state vector.

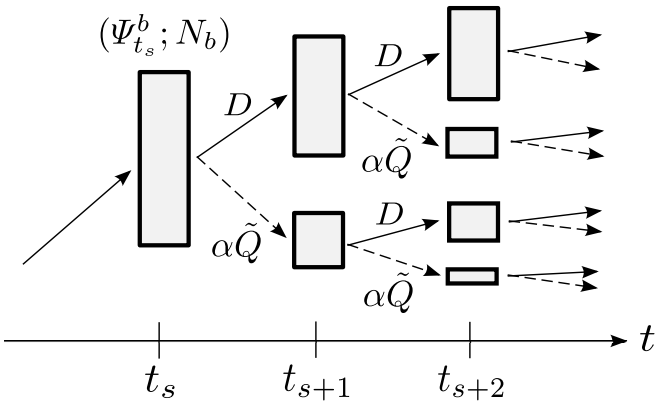

FIG. 1: Illustration of the one-space scheme. At time t_s a given block $(\Psi^b_{t_s}; N_b)$ containing N_b identical state vectors $\Psi^b_{t_s}$ is splitted due to the parallel action of the drift (arrows) and the jumps (dotted arrows). Here we have used only a single jump operator $\alpha\tilde{Q}$; each supplementary jump channel would need an additional dotted arrow.

Note that the operators D and $\tilde{Q}_j$ in Eq. (15) depend on the density matrix $\rho(t_s)$, which needs to be evaluated as the ensemble average in Eq. (16) (with t_s instead of $t_s + \Delta t$). The sum over all blocks in the ensemble averaging procedure (16) implies that all trajectories, or blocks of trajectories, become coupled, which is a characteristic of the simulation of nonlinear master equations.

For the two-space process, we proceed similarly but now each block $(|\Psi^b_{t_s}\rangle; N_b)$ is associated with another block $(|\Phi^b_{t_s}\rangle; N_b)$. Both undergo the same drift. For the multichannel jumps, we have to consider that each channel can undergo two types of jumps, namely $\alpha_j \tilde{Q}_j$ or $\alpha_j Q_j$, occurring with equal probabilities (see Sec. II B). Contrary to the one-space process, a given block b produces here two new blocks per jump channel j. The density matrix is reconstructed through

$$\begin{aligned}\rho(t_s + \Delta t) = \frac{1}{2} \sum_b \Big(& w_b |\Psi^b_{t_s+\Delta t}\rangle \langle \Phi^b_{t_s+\Delta t}| + \\ & w^*_b |\Phi^b_{t_s+\Delta t}\rangle \langle \Psi^b_{t_s+\Delta t}| \Big), \end{aligned} \tag{17}$$

where $w_b = (N_b/N) \langle \Psi^b_{t_s+\Delta t} | \Phi^b_{t_s+\Delta t} \rangle$.

3. Reinitialization procedure

As time goes on, additional blocks are generated and their number grows exponentially with time so that at the beginning the simulation is very fast, then becomes progressively slower, and finally converges to the situation where all state vectors evolve individually. The frequency at which the blocks are split depend on the total jump rate Γ. It is possible to reinitialize the state vectors

using the current density matrix to reduce the number of blocks to its minimum value, i.e. n, boosting the numerical time evolution considerably and setting the memory storage for the state vectors to its minimum.

III. HARMONIC OSCILLATOR

In order to test the validity of the proposed stochastic simulation schemes we study, as a first example, a quantum harmonic oscillator coupled to a classical heat bath at temperature T_e through a single coupling operator [17].

A. Basic equations

In terms of the position operator q and the momentum operator p, the Hamiltonian of an isolated particle of mass m in a harmonic potential $V(q) = m\omega^2 q^2/2$ is $H = p^2/2m + V(q)$, where ω is the angular frequency. This quantum oscillator is coupled to a heat bath assuming that the interaction is mediated through the position q of the particle as the only dissipative coupling operator, $Q_1 = q$. The dissipation rate introduced in Eq. (5) is given in terms of a simple scalar friction coefficient ζ_q,

$$M_e^q(T_e) = \frac{\zeta_q k_{\mathrm{B}} T_{\mathrm{e}}}{\hbar^2}. \tag{18}$$

When simulating the harmonic oscillator, it is quite natural to use the truncated energy eigenbasis $|k\rangle$, $k = 0, 1, \ldots, n-1$. Using the matrix representation of the position operator given by

$$q\,|k\rangle = \sqrt{\frac{\hbar}{2m\omega}}\Big(\sqrt{k}\,|k-1\rangle + \sqrt{k+1}\,|k+1\rangle\Big), \tag{19}$$

the truncation for $|k\rangle = |n-1\rangle$ is obtained by omitting the contribution $\sqrt{n}\,|n\rangle$. Knowing that the truncated diagonal Hamiltonian is $H\,|k\rangle = \hbar\omega(k+1/2)\,|k\rangle$, the momentum operator is obtained through the commutation relation $[q, H] = (i\hbar/m)p$ and the operator p_ρ occurring in the friction and jump operators is then computed by resorting to Eq. (13).

B. Stabilization procedure

1. Stopping criteria

For a one-space process with individually normalized trajectories, all trajectory weights w_b^l are constant at all times. Difficulties arise for stochastic processes normalized on average only, when the weights of state vectors vary over time. More precisely, with time the number of small blocks generated by the jumps increase exponentially and it can happen that the weights of a tiny fraction of them start dominating the propagation of the density matrix ρ. This fact, known as the exponential growth of the norm Felbinger1999,Ulrich2002,Breuer2004,Jacobs2009, leads to intractable statistical errors for times much smaller than the relaxation time. To track down the emergence of this instability, one can simply compute the contribution of the dominating state vectors $R(t) = \sum_{b\in G(t)} w_b(t) - R_0$, where $G(t)$ contains the 1% of all the state vectors having the largest weights $w_b^l(t)$ at time t. The offset R_0 is defined such that $R(0) = 0$. In our simulations we avoid instabilities by applying the reinitialization procedure (see Sec. II D 3) if R crosses a predefined upper bound R_c. After applying the reinitialization R can be imposed to restart from zero by adjusting the offset R_0 correspondingly. The numerical value of R_c depends on the structure of the stochastic equations and on the size of error bars one can afford. However, R itself depends only on the evolution of the distribution of the norm of the state vectors. This reinitialization procedure insures stable long time simulation.

For the two-space process one cannot uniquely define real positive weights and we therefore adopt the following one: $\widetilde{w}_b = \varpi_b / \sum_{b'} \varpi_{b'}$, where $\varpi_b = \langle \Phi_{t_s}^b | \Phi_{t_s}^b \rangle + \langle \Psi_{t_s}^b | \Psi_{t_s}^b \rangle$. Thereby R and G are analogously defined as for the one-space process by replacing w_b by $\widetilde{w}_b$. The definition of $\widetilde{w}_b$ permits to track the evolution of the norm of $|\Phi\rangle$ and $|\Psi\rangle$ simultaneously contrary to the absolute value of the overlap of $|\Phi\rangle$ and $|\Psi\rangle$.

2. Illustration

We now consider the relaxation of a quantum harmonic oscillator with $n = 10$ energy levels between the temperatures $k_{\mathrm{B}}T_e = (3/2)\hbar\omega$ and $k_{\mathrm{B}}T_e = (1/2)\hbar\omega$ using a dimensionless time step of $\omega\Delta t = 0.0001$ and $N = 2\cdot 10^5$ trajectories (see Fig. 2). We use a coupling constant of $\zeta_q = m\omega/10$ to be in the weak coupling regime. The large blocks represented by the ten plateaus generated by the initialization procedure at time $\omega t = 0$ are dissolved into the intermediate non-flat regions (see Fig. 2). For the harmonic oscillator simulated with the one-space process, we see that $R_c = 2$ induces a reinitialization after time intervals of $\omega t \simeq 2.0$ (the relaxation process takes some $\omega t \simeq 40.0$) giving a time evolution which coincides with the deterministic evolution (see Fig. 3). To reproduce the overlap of the three lowest energy eigenstates (see Fig. 4), it is necessary to use a lower bound $R_c = 1$, producing more frequent reinitialization every $\omega t \simeq 1.0$, because the range of values of the overlaps is much smaller than the range of the observables so that error bars have a bigger impact. At any fixed time the error bars become independent of R_c for $R_c < 0.5$. For the two-space process, we apply a boundary $R_c = 5$, which produces a first reinitialization after a time of $\omega t \simeq 0.5$, and indicates that the evolution becomes unstable much faster.

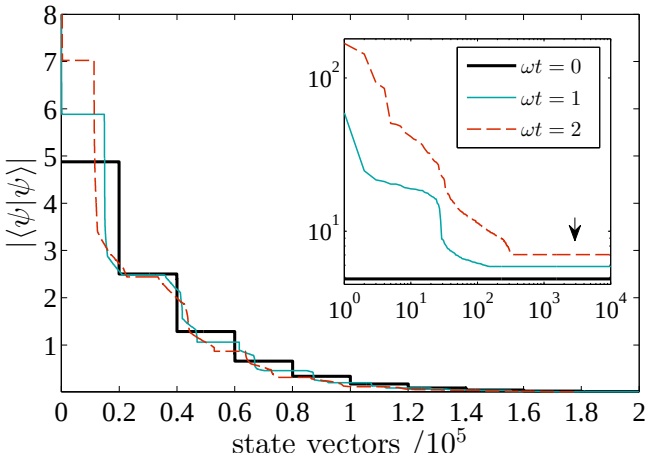

FIG. 2: Evolution of the norm $|\langle\Psi|\Psi\rangle| = N w_b^{l_b}$ proportional to the weight of the individual state vectors (ordered with decreasing weight from left to right) for a harmonic oscillator with $n = 10$ energy levels. The ten plateaus represent the large blocks generated by the initialization at $t = 0$. With time, the plateaus vanish due to the appearance of small blocks resulting from the random jumps. The insert shows a blow-up of the 1% of all the state vectors having the largest weights w_b^l (domain under the curves left of the arrow).

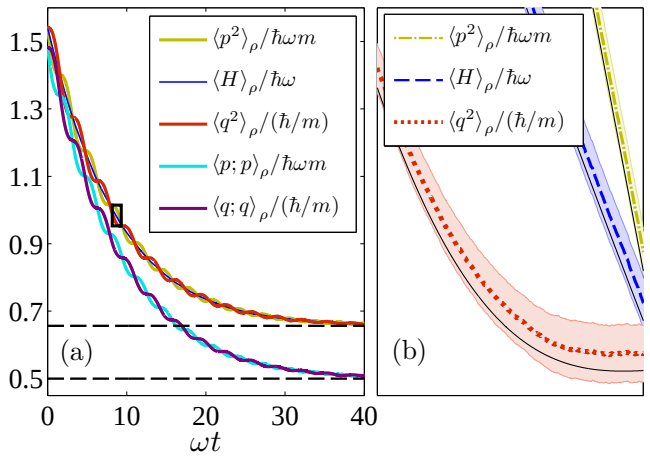

FIG. 3: Relaxation of a quantum harmonic oscillator coupled to a low temperature classical heat bath. (a) Evolution of averages (upper three curves) and canonical correlations (lower two curves); the dashed lines indicate the steady-state results. Subplot (b) is a blow-up of the marked area in (a) showing that the deterministic curves (thin black lines) lie in the shaded region representing the error bars of the order of 10^{-3} estimated from independent one-space stochastic runs.

C. Simulation results

To check whether the deterministic and simulation approaches agree, we initially thermalize the oscillator at $k_B T_0 = (3/2)\hbar\omega$, then immerse it in a heat reservoir with a lower temperature $k_B T_e = (1/2)\,\hbar\omega$, and let it relax to $\rho_{\rm eq} \propto \exp[-H/(k_B T_e)]$. For the integration of the deterministic nonlinear quantum master equation (given by Eq. (56) of [17]) we use the Euler scheme with a dimensionless time step $\omega\Delta t = 0.0001$. For the integration of the one-space stochastic process given by Eq. (1) we use the same time step and average over 20 independent runs, each of them containing $N = 2\cdot 10^5$ trajectories (see Sec. II D). As pointed out previously, we apply a reinitialization procedure (see Sec. III B). We follow the average of the observables q^2, p^2 and H (see Fig. 3) and the evolution of the overlap of some low energy eigenstates of the Hamiltonian with large probability eigenvectors of the density matrix (see Fig. 4). One can easily see that the two methods give consistent results for the one-space process within the error bars. The same holds for the two-space process.

We can numerically confirm some interesting features of the nonlinear master equation by using the stochastic process. We notice that the entropy production rate of the total system when considering a heat bath environment can be expressed in terms of the canonical correlation $\langle A;B\rangle_\rho = {\rm tr}(A_\rho B)$ such that [17]

$$\frac{dS_{\rm tot}}{dt} = \sum_j \frac{M_{\rm e}^{Q_j}(H_{\rm e})}{k_B {T_e}^2}\,\langle i[Q_j,F];i[Q_j,F]\rangle_\rho \geq 0, \quad (20)$$

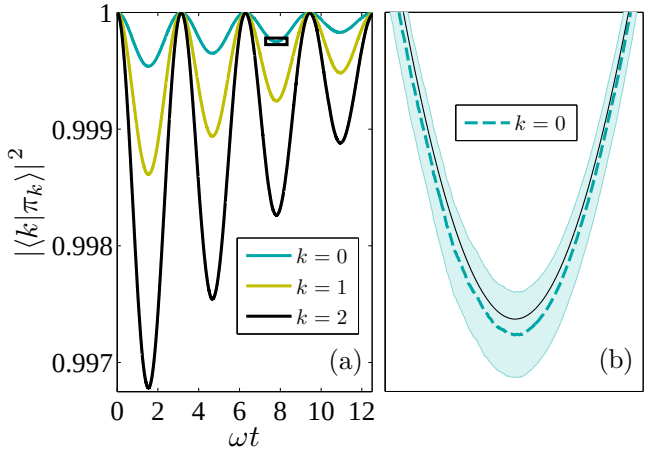

FIG. 4: Relaxation of a quantum harmonic oscillator coupled to a low temperature classical heat bath. (a) Overlap of three lowest energy eigenstates $|k\rangle$ with the three largest probability eigenvectors of the density matrix $|\pi_k\rangle$. Subplot (b) is a blow-up of the marked area in (a) showing that the deterministic curves (thin black line) lies in the shaded region representing the error bars of the order of 10^{-5} estimated from independent one-space stochastic runs.

where $F = H - T_e S$ is the Helmholtz free energy operator and $S = -k_B \ln\rho$ is the entropy operator associated with the von Neumann entropy. For the dissipation rate we use Eq. (18). Because the total entropy production rate is proportional to ${\rm tr}(A\rho^\lambda A^\dagger \rho^{1-\lambda})$ with $A = A^\dagger = i[Q_j, F]$, it is a convex functional on the state space of open systems due to Lieb's theorem on top of being non-negative and upper-bounded [3, 30, 31], i.e. $0 \leq \langle A;A\rangle_\rho \leq \langle A^2\rangle_\rho$.

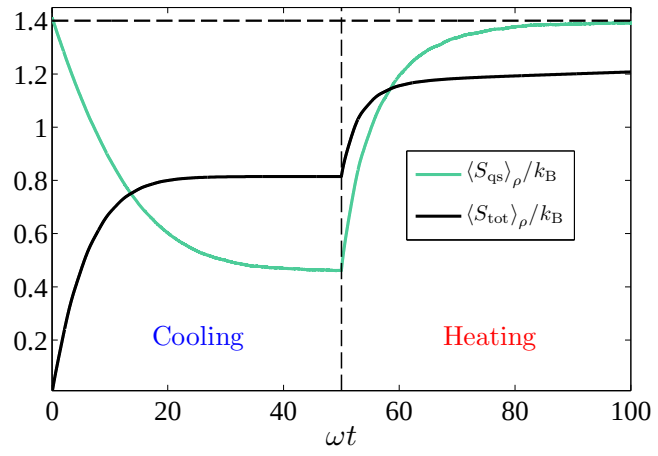

FIG. 5: Entropy evolution of a quantum harmonic oscillator coupled to a classical heat bath. Cycle composed of a cooling phase followed by a heating phase. The light-colored line stands for the quantum subsystem whereas the dark-colored one represents the composite quantum-classical system.

As a consequence of Eq. (20), the second law of thermodynamics is respected.

We examine the quantum oscillator starting from a temperature $k_{\rm B}T_0 = (3/2)\hbar\omega$ being cooled down to $k_{\rm B}T_1 = (1/2)\hbar\omega$ and then, at $\omega t = 50$, heated up back to the initial temperature to construct a thermodynamic cycle (see Fig. 5). We follow the evolution of the entropy of the quantum oscillator as well as of the total system and observe that the entropy of the quantum oscillator diminishes during the cooling phase while the total entropy increases (we set the initial total entropy equal to zero). Moreover, we see that the total entropy increase is larger during the cooling phase than during the heating phase as one would intuitively expect for such an irreversible process.

Further, we observe that, at equilibrium, the canonical correlations $\langle p;p\rangle_\rho$ and $\langle q;q\rangle_\rho$ converge to the thermal energy $k_{\rm B}T_e$ (the two lower curves in Fig. 3). This is a direct consequence of the fact that the second moment equation, which is equivalent to the master equation, fulfils a meaningful fluctuation-dissipation relation [12, 17]. This also implies that the evolution equation of averages (see Eq. (10) of [16]) strictly respect the Ehrenfest theorem, contrary to the Lindblad master equation [32].

IV. TWO-LEVEL SYSTEM

As a further test of the validity of the proposed stochastic simulation schemes we examine a two-level system coupled to a classical heat reservoir at temperature T_e through two coupling operators requiring the introduction of an additional jump channel compared to the harmonic oscillator.

A. Basic equations

For a two-level system or single qubit, the Hilbert space is commonly represented by the two-dimensional vector space $\mathbb{C}^2$. Observables acting on the corresponding quantum states can be expressed in terms of the three Pauli-matrices σ_1, σ_2 and σ_3 and the identity $\mathbb{I}$ playing together the role of basis vectors. In view of a concrete physical application especially focused on quantum optical systems [22, 33, 34], we choose the Hamiltonian $H = \hbar\omega\sigma_3/2$ separating the system's ground state and its excited state by an energy amount $\hbar\omega$. To take into account the interaction of the subsystem with the surrounding heat bath (assumed to be at temperature T_e), we use the transverse magnetization directions $Q_1 = \sigma_1/2$ and $Q_2 = \sigma_2/2$ as coupling operators. These describe for instance radiation transmitted between the two-level system and its surrounding [3]. To define dimensionless quantities we choose the Planck constant $\hbar$, the Boltzmann constant k_B and the frequency ω. The dissipation rate is assumed to be given by [17]

$$M_e^{Q_j}(T_e) = \zeta_0 \frac{k_{\rm B}T_{\rm e}}{\hbar\omega}\,, \quad j = 1, 2, \tag{21}$$

with ζ_0 the spontaneous emission rate γ_0 characterizing the strength of the interaction between the two-level system and the environment.

B. Detailed simulation results

To solve the thermodynamic quantum master equation in the framework of our stochastic simulation technique, we proceed in a similar way as for the harmonic oscillator (see Sec. III). The only difference is that we need two jump channels, one for each coupling operator. To check the proper convergence of the simulation results we can use the equilibrium solution of the quantum master equation being of the Boltzmann form. Consequently, the transverse magnetization and the mean energy approaches their proper equilibrium values, i.e., $\langle\sigma_{\hbar\omega,2}\rangle_\rho \to 0$ and $\langle H\rangle_\rho \to -(1/2)\tanh(\hbar\omega/2k_{\rm B}T_e)$.

To illustrate this, we examined the relaxation of a two-level system initially in a overpopulated state characterized by $\rho_0 = 1/10\,(5\,\mathbb{I} + 2\sigma_1 - \sigma_2 + \sigma_3)$. The temperature of the cold surrounding is given by $k_{\rm B}T_{\rm e} = 0.2\,\hbar\omega$, where $\hbar\omega$ is the level splitting and the spontaneous emission rate is chosen as $\gamma_0 = \omega/10$. We performed the integration of the deterministic nonlinear quantum master equation (given by Eq. (44) of [17]) with the Euler scheme with a dimensionless time step $\omega\Delta t = 0.005$. For the integration of the one-space stochastic process given by Eq. (1) we used the same time step and average over 60 independent runs, each of them containing $N = 5000$ trajectories (see Sec. II D). Simulation results, based on the one-space process, are illustrated in Fig. 6 and show the consistency of the deterministic and stochastic approaches. The one-space process does not require the ap-

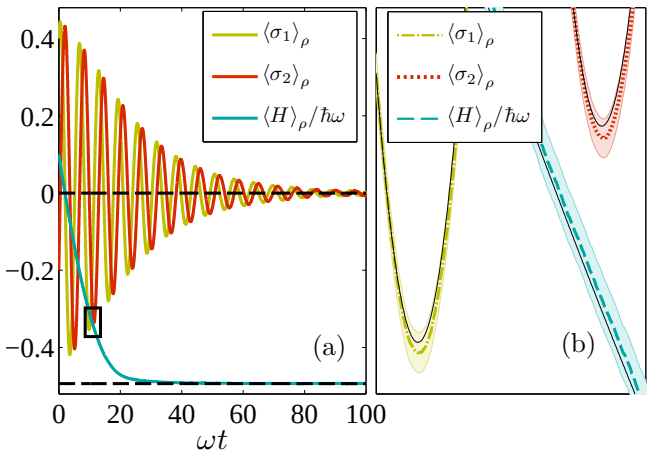

FIG. 6: Relaxation of a two-level system coupled to a low temperature classical heat bath. (a) Evolution of averages. Subplot (b) is a blow-up of the marked area in (a) showing that the deterministic curves (thin black lines) lie in the shaded region representing the error bars of the order of 10^{-3} estimated from independent one-space stochastic runs.

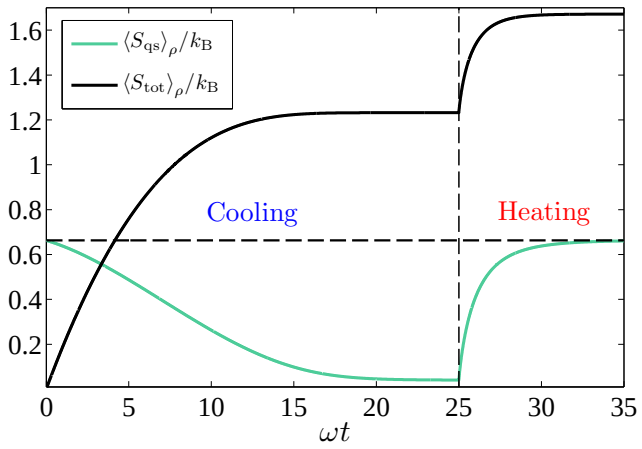

FIG. 7: Entropy evolution of a quantum two-level system coupled to a classical heat bath. Cycle composed of a cooling phase followed by a heating phase. The light-colored line stands for the quantum subsystem whereas the dark-colored one represents the composite quantum-classical system.

plication of the reinitialization strategy because α_j given by Eq. (7) leads to a stable evolution up to the time the system has relaxed. Nevertheless, one can reduce the error bars significantly by choosing $R_c = 2$ inducing around 3 reinitializations to reach equilibrium (relaxation time is $\omega t \simeq 100.0$). For the two-space process the evolution becomes unstable even when using α_j given by Eq. (12). Hence, for a proper relaxation it is necessary to apply the reinitialzation procedure. To reproduce the time evolution we have used $R_c = 1$ inducing a first reinitialization after an elasped time of $\omega t \simeq 4.0$.

As for the quantum harmonic oscillator (cf. Fig. 5), we examine the entropy production for a cooling-heating cycle with a cold reservoir at $k_{\rm B}T_0 = 0.2\,\hbar\omega$ and a hot reservoir at $k_{\rm B}T_1 = 2.0\,\hbar\omega$ showing a perfectly monotonic increase of the total entropy.

V. DISCUSSION

We carefully examined a thermodynamically inspired extension of usual stochastic unraveling processes [3] relying on a nonlinear thermodynamic quantum master equation [18] by studying two standard quantum systems: the two-level system and the harmonic oscillator. We have shown that the application of a reinitialization procedure splitting the time evolution into successive short time simulations insures that the unraveling procedure works perfectly fine although the norm of the simulated trajectories is only conserved on average.

It is worth to notice that this method is not restricted to the studied nonlinear stochastic process. On the contrary, it can be applied to any situation where the normalization is not intrinsically controlled [14, 23–25], for instance in the non-Markovian case or when resorting to a doubled Hilbert space (as for the two-space process presented in Sec. II B) where obtaining normalized equations is far from being a trivial task. The only requirement is to diagonalize the density matrix when the system starts to be unstable to be able to regenerate the state vectors from the current density matrix.

Because most of the trajectories of the studied stochastic process evolve similarly, we proposed an efficient implementation of the stochastic process where the reinitialization can be used to speed up the simulation and reduce the needed memory storage for the state vectors. To avoid the diagonalization involved in the reinitialization procedure, we can alternatively enlarge the blocks of the set G to dilute their weights so that in the following steps many tiny jumps will take place instead of few big ones inducing a more stable time evolution. When $R > R_c$ we increase the size of the blocks $b \in G$ by a factor η and rescale the corresponding state vectors $\left|\Psi^b_{t_s}\right\rangle$ by $\sqrt{\eta}$ to leave the density matrix unchanged. R is decreased by an approximate factor η. These techniques can be applied to any stochastic process and are opposite to the "branching" technique [35, 36] which eliminates the state vectors having a negligible contribution at the expense of obtaining an approximate density matrix.

The discussed nonlinear unraveling reaches the asymptotic equilibrium state for any kind of Hamiltonian because the nonlinear master equation was derived for very general systems [12]. On the one hand, we would like to emphasize that the relaxation to the asymptotic equilibrium state for the present unraveling is mainly ensured by the nonlinear structure of the equation and not through the specific damping coefficients. On the other hand, for the Lindblad quantum master equation, proper linear combinations of damping coefficients and coupling operators are crucial for relaxing to the correct equilibrium state; even to construct a proper process for two

qubits with an interaction term is very difficult [37, 38]. As a check, we simulated an anharmonic oscillator modeled by a Kerr term $\lambda(a^\dagger a)^2$, so that the Hamiltonian still possesses the same eigenstates $|n\rangle$, with the same damping coefficients as before. The system was found to relax towards equilibrium as expected.

The positivity of the density matrix is guaranteed for the one-space process because we can reconstruct the nonlinear master equation from the stochastic process through $\mathrm{E}\big(|\psi_t\rangle\langle\psi_t|\big)$ [3]. It is a remarkable feature of the one-space process that positivity can be guaranteed even after introducing arbitrarily large time steps for the purpose of numerical simulations (this is contrary to the usual deterministic integration schemes). We have shown that, for a Kerr oscillator with $n = 10$, the nonlinear master equation when solved numerically with a deterministic Euler or fourth-order Runge-Kutta scheme for increasing λ more quickly produces negative eigenvalues, even for small time steps. Hence, the stochastic approach possesses a higher robustness compared to the deterministic one. Furthermore, at the level of thermodynamics, it is especially noteworthy that for a quantum system coupled to a heat reservoir the total energy is conserved and that a positive entropy production is guaranteed. On top of that, evolution equations of averages are perfectly compatible with the Ehrenfest theorem.

As discussed in Sec. III B, it may be wise not to have too wild jumps to limit the increase of the norm of the individual state vectors. Because the precise structure of the jump and friction operators given by Eq. (2) and (3) is not crucial as long as they permit to recover the second moment equation, we can push the nonlinear term out of the jump operator $\tilde{Q}_j = \alpha_j Q_j$ and rewrite the friction operator as $\Lambda_j = (\gamma/2)(\mathbb{I} - {\alpha_j}^2 {Q_j}^2 - 2{\alpha_j}^2 \beta_j \left[Q_j, H\right]_\rho \rho^{-1})$. These settings allow to relax the oscillator to equilibrium with fewer applications of the reinitialization procedure. This clearly shows that different stochastic formulations are not equivalent for the numerical implementation [26].

In attempt to improve the stability of the two-space process, we have reexpressed it in a different perspective: we imposed a purely reversible drift by transferring the friction operator into the jump part which then carries all irreversibility. We tried various combinations of jump channels and jump operators. However, none of these combinations allowed to relax the subsystem to equilibrium without the reinitialization procedure. Nevertheless, we observed that the different unravelings possess specific time evolution of R and the ones exhibiting a slower increase are more stable. Therefore R can be used to characterize the numerical stability of a given stochastic process.

VI. CONCLUSION

The present unraveling producing the nonlinear thermodynamic master equation [12, 16, 17] will in the future permit to study many problems of great interest like entanglement in quantum information theory [2], nonlinear optical setups [4], superconducting qubit, nanomechanical resonators, cold atoms [1, 5], or dissipative quantum field theory [39]. It will also open the door to go beyond heat bath environments (like classical spins or oscillators) as well as allowing feedback effects from the environment through the dissipative brackets [16, 18]. Moreover, the unraveling methodology introduced in the companion paper [18] could allow to construct unravelings for many different master equations as we have shown briefly at the end of Sec.II A where we unravel for example the Caldeira-Leggett master equation.

[1] E. Wolf, *Nanophysics and Nanotechnology* (Wiley, Berlin, 2006), 2nd ed.
[2] M. Nielsen and I. Chuang, *Quantum Computation and Quantum Information* (Cambridge University Press, Cambridge, 2000).
[3] H.-P. Breuer and F. Petruccione, *The Theory of Open Quantum System* (Oxford University Press, Oxford, 2002).
[4] D. Walls and G. Milburn, *Quantum Optics* (Springer, Berlin, 2008), 2nd ed.
[5] U. Weiss, *Quantum Dissipative Systems*, vol. 13 (World Scientific, Singapore, 2008), 3rd ed.
[6] H.-P. Breuer and F. Petruccione, in *Irreversible Quantum Dynamics* (Springer, Berlin, 2003), vol. 622 of *Lecture Notes in Physics*, pp. 65–79.
[7] A. G. Redfield, IBM J. Res. Dev. **1**, 19 (1957).
[8] G. Lindblad, Commun. Math. Phys. **48**, 119 (1976).
[9] V. Gorini, A. Kossakowski, and E. C. G. Sudarshan, J. Math. Phys. **17**, 821 (1976).
[10] A. O. Caldeira and A. J. Leggett, Ann. Phys. (N.Y.) **149**, 374 (1983).
[11] W. J. Munro and C. W. Gardiner, Phys. Rev. A **53**, 2633 (1996).
[12] H. Grabert, Z. Physik B **49**, 161 (1982).
[13] A. Ishizaki and G. R. Fleming, J. Chem. Phys. **130**, 234110 (2009).
[14] K. Jacobs, Europhys. Lett. **85**, 40002 (2009).
[15] M. Nakatani and T. Ogawa, J. Phys. Soc. Jpn. **79**, 084401 (2010).
[16] H. C. Öttinger, Europhys. Lett. **94**, 10006 (2011).
[17] H. C. Öttinger, Phys. Rev. A **82**, 052119 (2010).
[18] H. C. Öttinger, Companion paper (2012).
[19] N. Gisin and I. C. Percival, J. Phys. A: Math. Gen. **25**, 5677 (1992).
[20] W. T. Strunz, L. Diósi, and N. Gisin, Phys. Rev. Lett. **82**, 1801 (1999).
[21] J. Dalibard, Y. Castin, and K. Mølmer, Phys. Rev. Lett. **68**, 580 (1992).
[22] H. Carmichael, *An Open Systems Approach to Quantum Optics*, Lecture Notes in Physics (Springer, Berlin, 1993).
[23] T. Felbinger and M. Wilkens, J. Mod. Opt. **46**, 1401 (1999).

[24] U. Kleinekathöfer, I. Kondov, and M. Schreiber, Phys. Rev. E **66**, 037701 (2002).
[25] H.-P. Breuer, Eur. Phys. J. D. **29**, 105 (2004).
[26] D. Lacroix, Phys. Rev. A **72**, 013805 (2005).
[27] G. J. Milburn, Phys. Rev. A **44**, 5401 (1991).
[28] B. C. Carlson, Amer. Math. Monthly **79**, 615 (1972).
[29] K. B. Stolarsky, Math. Mag. **48**, 87 (1975).
[30] G. Roepstorff, Commun. Math. Phys. **46**, 253 (1976).
[31] H. Spohn, J. Math. Phys. **19**, 1227 (1978).
[32] R. Karrlein and H. Grabert, Phys. Rev. E **55**, 153 (1997).
[33] H. M. Wiseman and G. J. Milburn, Phys. Rev. A **47**, 1652 (1993).
[34] K. Mølmer and Y. Castin, Quantum Semiclass. Opt. **8**, 49 (1996).
[35] K. Jacobs, Phys. Rev. A **81**, 042106 (2010).
[36] M. R. Hush, A. R. R. Carvalho, and J. J. Hope, Phys. Rev. A **80**, 013606 (2009).
[37] A. Isar and A. Sandulescu, arXiv:quant-ph/0602149v1 (2006).
[38] M. Scala, R. Migliore, and A. Messina, J. Phys. A: Math. Theor. **41**, 435304 (2008).
[39] H. C. Öttinger, Phys. Rev. D **84**, 065007 (2011).